Biomacromolecules

Subscriber access provided by Karolinska Institutet, University Library

Article

Synthesis and characterization of dendrimer-based polysarcosine star polymers: well-defined, versatile platforms designed for drug delivery applications

Richard M. England, Jennifer Hare, Anders Gunnarsson, Jeremy Stephen Parker, and Marianne B. Ashford

Biomacromolecules, **Just Accepted Manuscript** • DOI: 10.1021/acs.biomac.0c00768 • Publication Date (Web): 16 Jul 2020

Synthesis and characterization of dendrimer-based polysarcosine star polymers: well-defined, versatile platforms designed for drug delivery applications

*Richard M. England,[‡,†] * Jennifer I. Moss,[§] Anders Gunnarsson,[¥] Jeremy S. Parker,[†] and Marianne B. Ashford.[‡]*

[‡]Advanced Drug Delivery, Pharmaceutical Sciences, R&D, AstraZeneca, Macclesfield, UK.

[†]Early Chemical Development, Pharmaceutical Sciences, R&D, AstraZeneca, Macclesfield, UK.

[§]Early TDE, Oncology R&D, AstraZeneca, Cambridge, UK,

[¥]Discovery Sciences, Pharmaceutical Sciences, R&D, AstraZeneca, Gothenburg, Sweden.

KEYWORDS, dendrimer, star polymer, drug delivery, nanomedicine, Polymer Therapeutics, polysarcosine, N-carboxyanhydride, stealth polymer, lysine, branched polymer, ring opening polymerization, linker chemistry, SN-38.

ABSTRACT

This paper describes the synthesis of star polymers designed for future drug delivery applications. A generation-5 lysine dendrimer was used as a macroinitiator for the ring opening polymerization of sarcosine N-carboxyanhydride monomer to produce 32-arm star polymers with narrow molar mass distributions and desirable hydrodynamic size control. Fluorescent dye labeled polymers were dosed in mice to measure plasma pharmacokinetics. Long circulation times were observed, representing ideal properties for biophysical targeting of tumors. *In vivo* efficacy of one of these star polymers conjugated to the therapeutic molecule SN-38 was evaluated in mice bearing SW620 xenografted tumors to demonstrate high anti-tumor activity and low body weight loss compared to the SN-38 prodrug, irinotecan, and show the potential of these delivery

systems. As a further build, we demonstrated that these star polymers can be easily chain-end functionalized with useful chemical moieties, giving opportunities for future receptor targeting strategies. Finally, we describe the synthetic advantages of these star polymers that make them attractive from a pharmaceutical manufacturing perspective and report characterization of the polymers with a variety of techniques.

INTRODUCTION

When designing novel polymer-based drug delivery systems for translation into the clinic, there are many considerations to take into account before and during development.[1-6] From a platform perspective, important features for polymer carriers include: synthetic reproducibility, low toxicity/immunogenicity, a suitable clearance mechanism/biodegradability and capacity for high drug loading. Other considerations should include ease of manufacture, formulation, analytical characterization as well as low cost of goods. For drug delivery to tumors by biophysical targeting, the approach is typically to develop technologies with long

residence times in circulation to enable better tumor uptake,[7] and to limit release of an active drug in the circulation so to minimize non-target organ accumulation. To prolong systemic retention, the technology should avoid renal clearance by having a hydrodynamic size above the threshold for filtration and minimize the liver, spleen and lung accumulation by having properties to reduce scavenger cell uptake and resulting off-target toxicity.[8] The latter is normally controlled by addition of polymers and depends on polymer type, surface charge, hydrophilicity, hydrodynamic size and protein binding. Recent work has shown that nanoparticles of 20-30 nm with poly(ethylene glycol) (PEG), poly(sarcosine) (PSar) or poly(N-hydroxypropylmethacrylamide) (pHPMA) as the hydrophilic shells displayed negligible protein binding after incubation in human plasma and all showed prolonged blood circulation times when tested in mice.[9] Whilst PEG and pHPMA are well studied for *in vivo* drug delivery applications, PSar is now quickly emerging as an interesting polymer and a suitable alternative for both polymers. PSar is conveniently synthesized from the ring opening polymerization of sarcosine N-carboxyanhydride (NCA) which can be initiated from nucleophilic

groups typically under ambient conditions. This provides an advantage over PEG, which is typically purchased from commercial sources for most applications thus is more challenging to tailor structures or deliver copolymers with specific numbers of repeat units for a specific purpose. Additionally, there is growing evidence that anti-PEG antibodies can lead to accelerated clearance of PEGylated drug delivery systems upon repeated dosing, thus reducing their efficacy and increasing their accumulation in off-target clearance organs, leading to adverse effects.[10] PSar is proving to be a versatile material and has been used in many applications as a novel material, as comprehensively reviewed by Birke, Ling and Barz.[11] Interest is growing in the use of PSar for *in vivo* applications including: antibody and protein modification,[12, 13] tumor imaging,[14] peptide-based nanotubes,[15] polyplexes,[16] gold nanoparticles,[17] liposomes,[18] and micelles.[19, 20] In one of these reports, PSar modification of a therapeutic protein was shown to improve efficacy when tested in tumor-bearing animals when compared to PEG.[13] There are a small number of reports using amine-functional dendrimers as macroinitiators for the polymerization of sarcosine NCA to give well-defined, star-

shaped materials.[21-23] This approach offers a facile route to high molar mass material with functionality maintained on the polymer chain ends. However, these reports described the use of poly(trimethyleneimine) and poly(amidoamine) dendrimer cores, which retain cationic charge near the core. An overall cationic charge on a nanoparticle can be detrimental to drug delivery systems, where prolonged blood circulation is required, because of strong interactions with cell membranes.[8, 24] A further more recent example of a dendrimer used to polymerize PSar encompassed a generation 2 poly(propyleneimine) dendrimer to synthesize 8-arm star block copolymers of poly(benzyl-L-glutamate) and PSar.[25] The resulting amphiphilic structures formed nanoaggregates in water and were intended for crossing mucosal barriers for the delivery of therapeutics. This general approach to synthesizing star polymers, whilst more costly or time consuming in terms of synthetic steps of the dendrimer core, offers many benefits in terms of precision of the end product. This seems to be true for another type of star polymer involving the grafting-to approach of modifying dendrimer with pHPMA, where well-defined drug delivery systems could be synthesized and

applied.[26-28] Furthermore, star polymers may provide advantages over linear equivalents for drug delivery due to structural organization with increasing numbers of arms, and less overlapping at higher concentrations due to osmotic repulsion. [29, 30]

We previously reported on the synthesis of an L-lysine dendrimer modified with different poly(2-alkyl-2-oxazoline)s, designed to improve cytocompatibility.[31] One of these systems, with a poly(2-methyl-2-oxazoline) modification was tested for *in vivo* efficacy to deliver SN-38, an anticancer drug.[32] These experiments added to growing evidence that poly(2-methyl-2-oxazoline) is another alternative to the gold standard of drug delivery, PEG, that has also been extensively investigated as a modifier for dendrimers.[33-36] Indeed, docetaxel conjugated to a generation-5 lysine dendrimer modified with PEG, developed by StarPharma has progressed into Phase 2 clinical trials (EudraCT Number: 2016-000877-19). Here, we were interested to try a different "stealth" polymer to offer benefits in terms of the practicality of synthesis while maintaining the capability previously described for use as a flexible drug delivery system.[32] PSar is attractive because it can be

polymerized directly from the surface of the dendrimer. In this article we describe a scalable method for the synthesis of 32-arm star polymers from a lysine dendrimer “macroinitiator” with different PSar chain lengths. The potential of these star polymers to be used as a biophysical targeted drug delivery systems was investigated by comparing plasma pharmacokinetic data and evaluating the anti-tumor efficacy of one star polymer conjugated to the clinically relevant drug SN-38 *via* a hydrolytically cleavable linker. These star polymers offer numerous advantages for drug delivery applications, including precise sites for drug conjugation, facile control over chain length, control of hydrodynamic size and chain end functionality, which can be used to introduce targeting ligands onto the surface of the nanocarrier. This approach also offers a convenient purification by precipitation and filtration making it attractive from a manufacturing perspective. Finally, we examine a new characterization technique, mass photometry, as a convenient technique to give rapid molar mass determination at nanomolar concentrations, that we believe will find more frequent use in the area of polymer therapeutics and nanomedicine.

MATERIALS AND METHODS

All materials were purchased from Sigma Aldrich unless stated. Sarcosine N-carboxyanhydride was sourced from Wuxi AppTec and recrystallized from EtOAc/Heptane prior to use. 4-(4,6-Dimethoxy-1,3,5-triazin-2-yl)-4-methylmorpholinium tetrafluoroborate (DMTMM.BF_4) was synthesized as previously reported.[37] 3-(Maleimido)propionic acid N-hydroxysuccinimide ester was purchased from FluoroChem Ltd. Acetic acid N-hydroxysuccinimide ester was purchased from Apollo Scientific Ltd. Bovine Serum Albumin MALDI-TOF-MS calibration kit was purchased from AB SCIEX Ltd. NativeMark protein ladder was purchased from ThermoFisher. Irinotecan hydrochloride was purchased from Carbosynth Ltd.

Instrumentation

Nuclear Magnetic Resonance (NMR). Spectra were recorded on either a Bruker Ultrashield AVIII 500 MHz fitted with a QCI cryoprobe or a Bruker Ultrashield AVIII 400

MHz spectrometer fitted with a BBFO probe. Both instruments were operated with Topspin3.5pl5 software. Spectra were integrated using MestReNova version 9.0.

Size Exclusion Chromatography Triple Detection Array (SEC-TDA). Molar masses were determined using a Malvern Panalytical OMNISEC system using a TSKgel Alpha 4000 (300 x 7.8 mm, 10 µm) and a TSKgel Alpha 2500 (300 x 7.8 mm, 7 µm) in series. The eluent used was 50 mM sodium phosphate + 100 mM sodium nitrate (pH 6.8). The system was calibrated with a single Malvern Panalytical PEO 24 kDa narrow standard and absolute molar masses determined using the refractive index and light scattering signals. OMNISEC software version 11.0 was used.

Dynamic light scattering (DLS). A Malvern Zetasizer® Nano ZS instrument with back scattering detector (173°, 633 nm laser wavelength) was used. The dispersant RI and viscosity were assumed to be that of water (n = 1.59 and η = 0.888 mPa·s). The sample RI was 1.59 and the temperature was set at 25°C. The hydrodynamic diameter (D_H) was reported as the intensity-weighted average after a minimum of twelve measurements per sample and in triplicate and was calculated by the software. Samples were made to concentrations of 5 mg/ml in PBS at pH 7.4 and were filtered

using a 0.2 μm syringe filter prior to measurement. Data was obtained using Malvern Zetasizer software version 7.12.

Matrix Assisted Laser Desorption/Ionization Time of Flight Mass Spectrometry (MALDI-TOF-MS). Data were recorded using a Bruker UltrafleXtreme™. Samples were prepared at 5 mg/mL in methanol. A matrix solution of super-DHB (commercially available 9:1 mixture of 2,5-Dihydroxybenzoic acid and 2-hydroxy-5-methoxybenzoic acid) was prepared at 40 mg/mL in THF. The matrix (1 μL) was applied to an MTP 384 polished steel target plate followed by sample (1 μL). Neighboring spots were spotted with Bovine Serum Albumin calibrant in Sinapinic acid as per supplier's protocol. Spectra were recorded using Bruker flexControl software version 3.4 and analyzed using Bruker flexAnalysis software version 3.4. In-built method LP_30-210 kDa was used and the mass range extended for the largest star polymer analyzed.

Taylor Dispersion Analysis was performed on a Malvern Viscosizer TD fitted with a coated capillary and 214 nm wavelength filter. Measurements were performed at 25°C and buffer viscosity set at 0.8905 cP. Samples were made up at 10 mg/ml in phosphate buffered saline and the calibrant, caffeine was made up at 1 mg/ml in Milli-Q water. The

pressures applied were 1500 mbar pressure for the calibration and 140 mbar for samples. Data were recorded in Malvern Viscosizer TD software version 2.20.

Mass photometry was performed on a Refeyn One mass photometry instrument (Refeyn Ltd, UK). All samples were dissolved in HBS-N buffer (10mM HEPES, pH=7.4, 150mM NaCl), diluted to 50 and 100 nM and analyzed using 60 sec acquisition time. Resulting histograms were fitted to Gaussian distributions using DiscoverMP (Refeyn Ltd, UK) to extract peak contrast. Contrast-to-mass conversion was achieved by calibration using NativeMark protein ladder. Three protein species (with specified masses) were fitted to corresponding Gaussians to extract a linear relation between mass and contrast (Supporting Figure S1).

In vivo work

All animal studies were conducted in accordance with UK Home Office legislation, the Animal Scientific Procedures Act 1986, and the AstraZeneca Global Bioethics policy. All experimental work is outlined in project licences 70/8894 and P0EC1FFDF, which have gone through the AstraZeneca Ethical Review Process. Female BALB/c

(BALB/cOlaHsd) or athymic nude mice were purchased from Envigo, UK. All mice weighed more than 18 g at the time of the first procedure.

Plasma pharmacokinetics

To determine the plasma pharmacokinetic profile of the three different size star polymers, naïve female BALB/c mice (n = 3 per size) were injected intravenously *via* the lateral tail vein with a single dose of Cy5-labeled, carboxyl functional SD100, SD56 or SD28 at 50 mg/kg. The star polymers were dissolved in physiological saline and were administered in an injection volume of 0.05 mL/10 g mouse weight. After dosing, serial live bleeds were collected at various time points (5 min, 2 h, 6 h, 24 h, 48 h, 72 h and 144 h post-dose) for determination of plasma levels of the Cy5-labeled star polymer. Briefly, 20 µL of blood was collected from the tail vein using capillary tubes. Blood was diluted with 80 µL of PBS and centrifuged at 19,000 xg for 4 min at 4°C. The supernatant was collected and stored at -80°C until analysis. For analysis, a calibration curve was prepared using serial dilutions of the dosing solutions in a 96-well plate. 40 µL samples from the live bleeds were plated as well. Fluorescent measurements were made using a CLARIOstar plate reader using the Cy5 pre-set. The measurement

parameters were: excitation = 610-30 nm; emission = 675-50 nm; dichroic filter = auto 637.5; gain = obtained by enhanced dynamic range; number of flashes = 20.

Anti-tumor efficacy in SW620 xenograft model in mice

The anti-tumor efficacy of SD100-SN38 was evaluated in the SW620 xenograft model in female nude mice. Mice were implanted subcutaneously in the left flank with 1 x 10^6 cells in 50% Matrigel. Tumor growth was monitored twice weekly using intersecting calliper measurements; tumor volume was calculated using 3.14*length*width^2/6000, where length is the longer dimension. Body weights were recorded at the time of tumor measurement, and daily if weight loss exceeded 8%. Mice were randomized based on tumor volume to ensure an equal volume distribution across groups; the average tumor volume at the start of dosing was ~0.240 cm^3. Mice (n = 7 mice/group) were dosed once weekly for 3 weeks with saline, irinotecan at 50 mg/kg or SD100-SN38 at 4 mg SN38/kg. Saline and SD100-SN38 were administered intravenously *via* the lateral tail vein; irinotecan was administered intraperitoneally. At 24 h after the final dose, 3 mice per group were euthanized *via* Schedule 1 method with secondary confirmation, and

tissues were excised, weighed and processed to determine the SN38 concentration in liver, spleen and tumor.

Analysis of SN-38 concentration in tumor, liver and spleen

Tissues were weighed and put into FastPrep Lysing Matrix A Tubes (MP Biomedicals UK). Three times the volume of water per tissue weight was added to the tissue for homogenization. The samples were homogenized using a FastPrep-24™ machine (MP Biomedicals UK) at 6 m/s for 45 seconds. The cycle was repeated twice to gain complete homogenization. Control tissue from undosed animals was homogenized as above and spiked with an 11 point standard calibration curve (1-10000 nM SN-38) prepared in DMSO. Tissue homogenates (25 µL) were precipitated with acetonitrile (100 µl) containing internal standard, followed by centrifugation at 4500 rpm for 10 minutes. The supernatant (50 µl) was then diluted in 300 µl water and analyzed *via* UPLC-MS/MS.

Synthetic procedures

Poly(L-Lysine) dendrimers. The synthetic procedures can be found in the supporting information.

SN-38 ester linker synthesis has been reported previously.[32] Release rate data and methodology can be found in the supporting information.

Synthesis of 4-(2-furylmethylamino)-4-oxo-butanoic acid. Succinic anhydride (1.7 g, 17 mmol) was added to a 250 mL round bottom flask and partially dissolved in dichloromethane (DCM) (25 mL) with stirring (400 RPM). Furfurylamine (1 mL, 11 mmol) was added drop-wise in 0.1 mL portions every 10 min. Almost immediately a thick precipitate formed that was stirred for 1 h following full addition of the amine. The precipitate was diluted with further DCM (50 mL) and filtered and then washed on the filter pad with additional DCM (2 x 15 mL). The white solid was dried overnight under vacuum at 40°C to yield the title compound. Yield = 1.03 g, 47 %. ^{1}H NMR (d_6-DMSO, 500 MHz): δ= 2.34 (t, COC**H**$_2$), δ= 2.34 (t, C**H**$_2$CO$_2$H), δ= 4.23 (d, NH-C**H**$_2$), δ= 6.37 (dd, Fur-**H**), δ= 6.62 (dd, Fur-**H**), δ= 7.55 (d, Fur-**H**), δ= 8.29 (-N**H**-), δ= 12.05 (t, CO$_2$**H**). ^{13}C NMR (d_6-DMSO, 500 MHz): δ= 28.99 (CO**C**H$_2$), δ= 29.81 (**C**OOH$_2$), δ= 35.46 (NH**C**H$_2$), δ= 106.63 (Fur-**C**H), δ= 110.38 (Fur-**C**H), δ= 141.96 (Fur-**C**H), δ= 152.37 (Fur-**C**-CH$_2$), δ= 170.83 (NH-**C**O), δ= 173.78 (**C**O$_2$H).

G5-PLL[P(Sar)$_{28}$]$_{32}$[boc]$_{32}$ (SD28Boc). Sarcosine NCA (4.5 g, 39 mmol) was weighed out into an oven-dried 100 mL Schlenk tube and fitted with a septum and purged with nitrogen for 10 minutes. Anhydrous DMF (20 mL) was added via syringe and stirred until the solid was fully dissolved. A solution of G5-PLL[NH_2]$_{32}$[boc]$_{32}$ (512 mg, 0.044 mmol) dissolved in anhydrous DMF (2 mL) was added *via* syringe in one rapid addition. The reaction was stirred overnight at room temperature with nitrogen flow. Methoxyacetyl chloride (0.261 mL, 2.79 mmol) was added *via* Eppendorf pipette followed by pyridine (0.226 mL, 2.79 mmol) and the reaction mixture stirred for 1 h at room temperature. The solution was added to a rapidly stirring mixture of ethyl acetate (360 mL) and ethanol (40 mL) to form a precipitate. The precipitate was vacuum filtered and dried for 30 minutes on the filter pad under nitrogen. The solid was re-dissolved in methanol (10 mL) and added drop-wise to a mixture of ethyl acetate (280 mL) and ethanol (20 mL) and the solid obtained by vacuum filtration and after drying at 40^{o}C in a vacuum oven for 24 h. Yield = 3.08 g, 91.5 %. ^{1}H NMR (500 MHz, D_2O) 1.04 – 1.98 (374H, br), 2.61 – 3.22 (2814H, br), 3.27 – 3.41 (94H, br), 3.87 – 4.55 (1896H, br).

G5-PLL[P(Sar)$_{56}$]$_{32}$[boc]$_{32}$ (SD56Boc). Method as for compound G5-PLL[P(Sar)$_{28}$]$_{32}$[boc]$_{32}$ (SD28). Reagent quantities: Sarcosine NCA (4.5 g, 39 mmol), G5-PLL[NH$_2$]$_{32}$[boc]$_{32}$ (256 mg, 0.022 mmol), methoxyacetyl chloride (120 µL, 1.284 mmol), pyridine (104 µL, 1.284 mmol). Yield = 2.94 g, 95.7%. ^{1}H NMR (500 MHz, D_2O) 1.04 – 1.98 (374H, br), 2.61 – 3.22 (5891H, br), 3.27 – 3.41 (102H, br), 3.87 – 4.55 (3945H, br).

G5-PLL[P(Sar)$_{100}$]$_{32}$[boc]$_{32}$ (SD100Boc). Method as for compound G5-PLL[P(Sar)$_{28}$]$_{32}$[boc]$_{32}$ (SD28). Reagent quantities: Sarcosine NCA (3.13 g, 27.2 mmol), G5-PLL[NH$_2$]$_{32}$[boc]$_{32}$ (100 mg, 0.0085 mmol), methoxyacetyl chloride (38 µL, 0.411 mmol), pyridine (33 µL, 0.411 mmol). Yield = 1.96 g, 95.5%. ^{1}H NMR (500 MHz, D_2O) 1.04 – 1.98 (374H, br), 2.61 – 3.22 (10728H, br), 3.27 – 3.41 (94H, br), 3.87 – 4.55 (7123H, br).

G5-PLL[P(Sar)$_{28}$]$_{32}$[NH$_2$.TFA]$_{32}$ (SD28). SD28Boc (3.5 g, 0.045 mmol) was suspended in DCM (18 mL) under nitrogen flow. TFA (9 mL) was added dropwise over 5 minutes and the reaction was stirred for 2 h at room temperature. The reaction mixture was added to rapidly stirring TBME (400 mL) to form a precipitate. The solid was collected

by vacuum filtration and dried for 1 h on the filter pad under nitrogen flow. The solid was dried in a vacuum oven at 40°C overnight and then freeze-dried for 48 h from Milli-Q water (30 mL) to give the title compound. Yield = 2.84 g, 0.037 mmol). ^{1}H NMR (400 MHz, D_2O) 1.04 – 1.98 (374H, br), 2.61 – 3.22 (2814H, br), 3.27 – 3.41 (94H, br), 3.87 – 4.55 (1896H, br).

G5-PLL[P(Sar)$_{56}$]$_{32}$[NH$_2$.TFA]$_{32}$ (SD56). The method was followed as for SD28 starting from 2.8 g of SD56Boc. Yield = 2.5 g, 91.0 %. ^{1}H NMR (500 MHz, D_2O) 1.04 – 1.98 (374H, br), 2.61 – 3.22 (5891H, br), 3.27 – 3.41 (102H, br), 3.87 – 4.55 (3945H, br).

G5-PLL[P(Sar)$_{100}$]$_{32}$[NH$_2$.TFA]$_{32}$ (SD100). The method was followed as for SD28 starting from 1.9 g of **SD100Boc**. Yield = 1.75 g, 85.1 %. ^{1}H NMR (400 MHz, D_2O) 1.04 – 1.98 (374H, br), 2.61 – 3.22 (10728H, br), 3.27 – 3.41 (94H, br), 3.87 – 4.55 (7123H, br).

Reaction time course and end group modifications:

G5-PLL[P(Sar)$_{56}$-NH$_2$]$_{32}$[boc]$_{32}$ (SD56Boc-NH$_2$). Sarcosine NCA (1.47 g, 12.8 mmol) was added to an oven-dried Schlenk tube fitted with a septum. The solid was purged with nitrogen and anhydrous DMF (8 mL) was added *via* syringe. A solution of G5-

$PLL[NH_2]_{32}[boc]_{32}$ (85 mg, 0.007 mmol) dissolved in anhydrous DMF (0.5 mL) was added in one rapid addition *via* syringe. Aliquots of the reaction mixture (100 µL) were taken every 30 minutes for 3.5 h and added to ethyl acetate (12 mL) in 15 mL Falcon tubes to form a precipitate. The precipitate was agitated and centrifuged at 2800 xg for 5 minutes. The obtained solids were dried under vacuum at 40°C for 24 h. The remaining reaction was stirred overnight and added to a rapidly stirring ethyl acetate (100 mL) to form a precipitate. The solid was collected by vacuum filtration and dried overnight in a vacuum oven at 40°C. Yield = 0.95 g, 96 %. The samples taken at different timepoints were evaluated by MALDI-TOF-MS and Mass Photometry. ^{1}H NMR (500 MHz, D_2O) 0.89 – 1.84 (594H, br), 2.29 – 2.46 (102H, br), 2.63 – 3.27 (5479H, br), 3.37 – 3.44 (19H, br), 3.67 – 3.72 (55H, br), 3.89 – 4.60 (3584H, br).

G5-PLL[P(Sar)$_{56}$-DBCO/Acetyl amide]$_{32}$[boc]$_{32}$ (SD56Boc-DBCO/Ac). G5-PLL[P(Sar)$_{56}$-$NH_2]_{32}[boc]_{32}$ (400 mg, 2.89 µmol) was dissolved in anhydrous DMF (3 mL). DIPEA (48 µL, 0.28 mmol) was added and the solution stirred briefly. A solution of Dibenzocyclooctyne-N-hydroxysuccinimidyl ester (DBCO-NHS) (10 mg, 24.9 µmol) in DMF (0.5 mL) was added and the reaction mixture stirred for 1 h at RT. Acetic acid N-

hydroxysuccinimide ester (20 mg, 127 μmol) was added as a solid and the reaction stirred for 1 h at RT. The reaction mixture was added dropwise to a stirred mixture of ethyl acetate (150 mL) and acetonitrile (50 mL) to form a precipitate. The precipitate was stirred for 15 minutes and then collected by vacuum filtration and washed with ethyl acetate (20 mL). The solid was dried for 30 minutes on the filter pad under nitrogen and then dissolved in Milli-Q water, filtered (0.45 μm PVDF) and freeze-dried to obtain the title compound. Yield = 345 mg, 84 %. ^{1}H NMR (400 MHz, D_2O) 0.89 – 1.82 (644H, br), 1.93 – 1.97 (17H, br), 2.06 – 2.12 (43H, br), 2.47 – 3.30 (5505H, br), 3.75 – 4.60 (3584H, br), 5.00 – 5.10 (25H, br), 7.12 – 7.79 (103H, br).

G5-PLL[P(Sar)$_{56}$-Maleimide]$_{32}$[boc]$_{32}$ (SD56Boc-Mal). G5-PLL[P(Sar)$_{56}$-NH$_2$]$_{32}$[boc]$_{32}$ (100 mg, 2.89 μmol) was dissolved in anhydrous DMF (2 mL). DIPEA (8 μL, 0.28 mmol) was added and the solution stirred briefly. A solution of N-succinimidyl 3-maleimidopropionate (Maleimide-NHS) (13 mg, 46.4 μmol) in DMF (0.5 mL) was added and the reaction mixture stirred for 2 h at RT. The reaction mixture was added to a rapidly stirring mixture of ethyl acetate (100 mL) and acetonitrile (100 mL) to form a precipitate. The suspension was stirred for 15 minutes and then filtered and freeze-dried

as for SD56Boc-DBCO/Ac above. Yield = 95 mg, 91.8 %. ^{1}H NMR (500 MHz, D_2O) 0.77 – 2.06 (624H, br), 2.56 – 3.38 (5693H, br), 3.61 – 3.75 (85H, br), 3.80 – 3.89 (38H, br), 3.89 – 4.58 (3584H, br), 6.67 – 6.87 (79H, br).

G5-PLL[P(Sar)$_{56}$-Biotin]$_{32}$[boc]$_{32}$ (SD56Boc-Biotin). G5-PLL[P(Sar)$_{56}$-NH$_2$]$_{32}$[boc]$_{32}$ (100 mg, 2.89 μmol) was dissolved in anhydrous N,N'-dimethylformamide (2 mL). DIPEA (8 μL, 0.28 mmol) was added and the solution stirred briefly. A solution of Biotin-NHS ester (16 mg, 46.9 μmol) in DMF (0.5 mL) was added and the reaction mixture stirred for 3 h at RT. The reaction mixture was added to a rapidly stirring mixture of ethyl acetate (100 mL) and acetonitrile (100 mL) to form a precipitate. The suspension was stirred for 15 minutes and then filtered and freeze-dried as for SD56Boc-DBCO/Ac above. Yield = 95 mg, 90.3 %. ^{1}H NMR (500 MHz, D_2O) 0.96 – 1.92 (714H, br), 2.30 – 2.38 (17H, br), 2.47 – 2.58 (34H, br), 2.75 – 2.82 (72H, br), 2.83 – 3.30 (5497H, br), 3.31 – 3.42 (45H, br), 3.99 – 4.47 (3584H, br), 4.49 – 4.68 (57H, br).

G5-PLL[P(Sar)$_{56}$-furfuryl]$_{32}$[boc]$_{32}$ (SD56Boc-furfuryl). G5-PLL[P(Sar)$_{56}$-NH$_2$]$_{32}$[boc]$_{32}$ (100 mg, 2.89 μmol) was dissolved in anhydrous N,N'-dimethylformamide (2 mL). DIPEA (8 μL, 0.28 mmol) was added and the solution stirred briefly. A premixed solution

of 4-(2-furylmethylamino)-4-oxo-butanoic acid (7.0 mg, 35.5 μmol) and DMTMM.BF_4 (16 mg, 46.33 μmol) in DMF (2 mL) was added and the reaction mixture stirred for 3 h at RT. The reaction mixture was added to a rapidly stirring mixture of ethyl acetate (100 mL) and acetonitrile (100 mL) to form a precipitate. The suspension was stirred for 15 minutes and then filtered and freeze-dried as for SD56Boc-DBCO/Ac above. Yield = 93 mg, 89.9 %. ^{1}H NMR (500 MHz, D_2O) 0.79 – 1.96 (563H, br), 2.39 – 2.53 (77H, br), 2.56 – 3.44 (5498H, br), 3.80 – 4.59 (3584H, br), 6.17 – 6.45 (54H, br), 7.33 – 7.50 (23H, br).

G5-PLL[P(Sar)$_{28}$]$_{32}$[Cy5]$_2$[COOH]$_{30}$ (SD28-Cy5-COOH). G5-PLL[P(Sar)$_{28}$]$_{32}$[NH_2.TFA]$_{32}$ (50 mg, 0.6 μmol) was dissolved in anhydrous DMF (2 mL) in a 10 mL round bottom flask and stirred to dissolve. DIPEA (14 μL, 0.08 mmol) was added followed by a solution of Cyanine 5 NHS ester (0.8 mg, 0.001 mmol) from a stock solution (4 mg/mL in DMF). The reaction mixture was stirred for 1 h at RT. A solution of succinic anhydride (4.1 mg, 0.041 mmol) from a stock of 40 mg/ml dissolved in DMF was added and the pH adjusted with additional DIPEA to pH8-9 (5 μL added to 5μL of Milli-Q water and tested on pH paper). The reaction mixture was stirred for 4 h at room temperature before being

added drop-wise to rapidly stirring TBME (45 mL) to form a blue precipitate. The solid was obtained by centrifuging at 3000 xg to obtain a blue pellet after decanting the solvent to waste. The solid was dried overnight at RT under vacuum (50 mBar). The solid was dissolved in Milli-Q water (0.5 mL) and the pH adjusted to 3-4 using 2 M HCl. The solution was passed through a Pierce™ Dextran desalting column (5 kDa MWCO) and early blue fractions collected. The fractions were frozen and freeze-dried before collating pure fractions. The title compound was obtained as a dark blue solid. Yield = 42 mg, 80 %. ^{1}H NMR (500 MHz, D_2O) 0.98 – 1.85 (364H, br), 3.23 – 3.60 (131H, br), 3.66 – 3.23 (2642H, br), 3.27 – 3.40 (91H, br), 3.86 – 4.55 (1792H, br).

G5-PLL[P(Sar)$_{56}$]$_{32}$[Cy5]$_2$[COOH]$_{30}$ (SD56-Cy5-COOH). The method for **SD28-Cy5-COOH** was followed but using G5-PLL[P(Sar)56]$_{32}$[NH_2.TFA]$_{32}$ (50 mg, 0.4 μmol), DIPEA (8 μL, 0.046 mmol), Cyanine 5 NHS ester (0.43 mg, 0.7 μmol) from a stock solution (4 mg/mL in DMF), succinic anhydride (2.3 mg, 0.023 mmol) (from stock solution of 40 mg/mL in DMF. Yield = 41 mg, 82 %. ^{1}H NMR (500 MHz, D_2O) 0.98 – 1.85 (329H, br), 3.23 – 3.60 (160H, br), 3.66 – 3.23 (5416H, br), 3.27 – 3.40 (100H, br), 3.86 – 4.55 (3584H, br).

G5-PLL[P(Sar)$_{100}$]$_{32}$[Cy5]$_2$[COOH]$_{30}$ (SD100-Cy5-COOH). The method for **SD28-Cy5-COOH** was followed but using G5-PLL[P(Sar)56]$_{32}$[NH_2.TFA]$_{32}$ (50 mg, 0.4 μmol), DIPEA (8 μL, 0.046 mmol), Cyanine 5 NHS ester (0.43 mg, 0.7 μmol) from a stock solution (4 mg/mL in DMF), succinic anhydride (2.3 mg, 0.023 mmol) (from stock solution of 40 mg/mL in DMF. Yield = 46 mg, 92%. ^{1}H NMR (500 MHz, D_2O) 0.98 – 1.85 (473H, br), 3.23 – 3.60 (276H, br), 3.66 – 3.23 (9876H, br), 3.27 – 3.40 (52H, br), 3.86 – 4.55 (6400H, br).

G5-PLL[P(Sar)$_{100}$]$_{32}$[SN-38]$_{32}$ (SD100-SN38). G5-PLL[P(Sar)$_{100}$]$_{32}$[NH_2.TFA]$_{32}$ (200 mg, 0.8 μmol) was dissolved in anhydrous DMF. TEA (10.8 μL, 0.08 mmol) was added. In a separate vial, 2-(4-(4-oxo-4-SN38 butyl)-1H-1,2,3-triazol-1-yl)acetic acid (19 mg, 0.032 mmol) and DMTMM.BF_4 (18 mg, 0.040 mmol) were dissolved in anhydrous DMF (1 mL) and then added slowly to the polymer containing solution. The reaction was stirred for 3 h at RT and then added drop-wise to rapidly stirring ethyl acetate (125 mL) to form a precipitate, which was collected by filtration. The solid was re-dissolved in methanol (3 mL) and added to a rapidly stirring mixture of 50/50 ethyl acetate/tetrahydrofuran. This process was repeated once more to give the title compound as a pale yellow solid. Yield

= 172 mg, 81 %. ^{1}H NMR (400 MHz, d4-acetic acid) 0.65 – 0.96 (110H, br), 1.24 – 1.35 (68H, br), 2.44 – 3.15 (9684H, br), 3.19 – 3.36 (168H, br), 3.46 – 4.87 (6400H, br), 5.06 – 5.64 (143H. br), 6.98 – 8.34 (109H, br).

RESULTS AND DISCUSSION

Synthesis and characterization of polysarcosine star polymers. A generation-5 lysine dendrimer (ε-boc protected) was used as a macroinitiator to polymerize sarcosine N-carboxyanhydride to give 32-arm star polymers with different chain lengths (Scheme 1). The polymerization was directed to the lysine α-amino groups with the boc-protected ε-amine positioned for further functionalization e.g. with drug-linker molecules after the polymerization to provide more precision for drug loading and ultimately better reproducibility, which are key drivers for pharmaceutical development. This controlled approach offered additional benefits, as a pre-synthesized and characterized linear polymer with bespoke end groups was not required, reducing reaction steps. The polymerization was performed at room temperature with carbon dioxide as the by-product, which was

removed as the reaction progressed by purging with nitrogen. This synthesis gave high yields of material after a simple process of precipitation of the product into an antisolvent (ethyl acetate/ethanol mixture), followed by filtration.

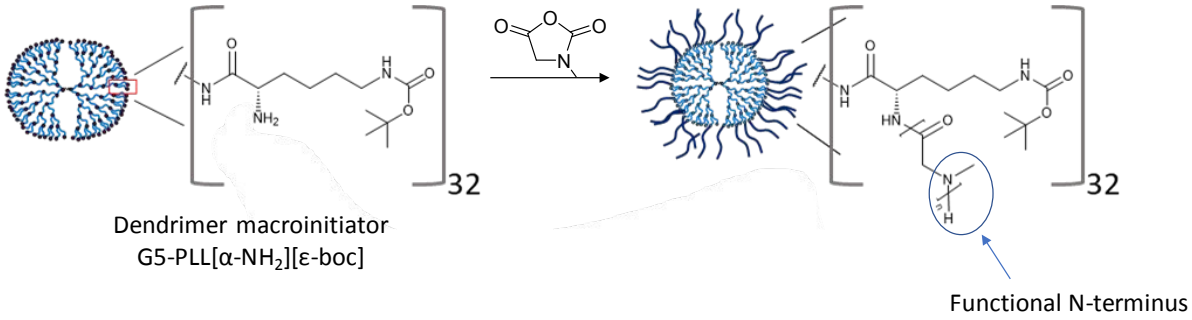

Scheme 1. Polymerization of sarcosine N-carboxyanhydride from generation 5 lysine dendrimer macroinitiator to give a 32-arm star polymer with terminal amino groups.

Previously, for the polyoxazoline-modified dendrimer, the excess linear polyoxazoline had to be removed by a diafiltration step to yield the pure star polymer before freeze-drying, adding to the technical challenge upon scale up.[31] An interesting finding for the polysarcosine star polymers was the excellent solubility in water, methanol, acetic acid, dimethylformamide and dimethyl

sulfoxide but poor to no solubility in several organic solvents, including ethers, ethyl acetate, tetrahydrofuran, acetonitrile and acetone. This allowed the removal of excess reagents, reaction solvent and low molar mass linear polysarcosine that may have formed *in situ*, during the precipitation into antisolvent. This strategy could also be used to remove excess drug-linker from a drug conjugation step, simplifying purification and making the process easier to scale. A useful attribute of using the dendrimer core to polymerize Sar-NCA was that the chain length, and therefore hydrodynamic size, could be tuned simply by altering the feed ratios of dendrimer macroinitiator and monomer (Table 1).

Table 1. Summary of characterization data for star polymers with degrees of polymerization of 28, 56 and 100.

Description	DP[a]	M_n (kDa)[b]	Đ[b]	Mass M_p (kDa)[c]	Inferred Molar Mass (kDa)[d]	DLS R_H (nm)	SEC R_H (nm)	Taylor Dispersion Analysis R_H (nm)
SD28	29	78.9	1.08	74.8	79 ± 9	5.1	4.5	5.8

SD56	58	149.3	1.09	140.2	149 ± 16	7.1	7.2	8.0
SD100	95	252.2	1.12	230.0	228 ± 25	9.1	8.3	9.3

[a]Degree of Polymerization from ^{1}HNMR. [b]SEC-TDA. [c]Peak Maximum molar mass from MALDI-TOF-MS. [d]Molar masses inferred from Mass Photometry.

PSar chain lengths of n= 28 and 56 were chosen based on molar mass equivalents to linear PEG (2000 g/mol and 4000 g/mol), which are amongst the most common PEGs used for drug delivery systems. A further nominal n= 100 sample was synthesized as the highest molar mass star polymer for investigation. These samples were denoted SD28, SD56, SD100, signifying PSar-modified dendrimer and the number of repeat units per chain. The amino terminal chain ends were capped with methoxyacetyl chloride yielding charge neutral, non-reactive methoxy terminal groups. The expected masses calculated from the relative molar ratios of dendrimer core and monomer were 77 kDa, 141 kDa and 241 kDa. The resulting star polymers were characterized by SEC-TDA (Figure 1A) and determined to have number average molar masses of 79 kDa, 149 kDa and 252 kDa, which were in close agreement with the expected masses.

Likewise, MALDI-TOF-MS analysis (Figure 1B) gave values of 75 kDa, 140 kDa and 230 kDa (relating to peak max values) and was also in close agreement. To characterize by ^{1}HNMR, the boc groups on the lysine core were first removed to help with integration of the dendrimer core (Figure 1C). Quantification of the chain-end methoxy group against the signals from sarcosine by ^{1}HNMR integration also gave the expected number of repeat units per chain. The molar mass dispersities of the star polymers were low (<1.15) for each example, with minimal high molar mass species, demonstrating good control of polymerization (Figure 1A). The hydrodynamic diameters of the star polymers were found to be 10, 14 and 18 nm as determined by Dynamic Light Scattering (DLS) (Figure 1D) and were in good agreement with the 9, 14 and 18 nm determined by SEC (Table 1).

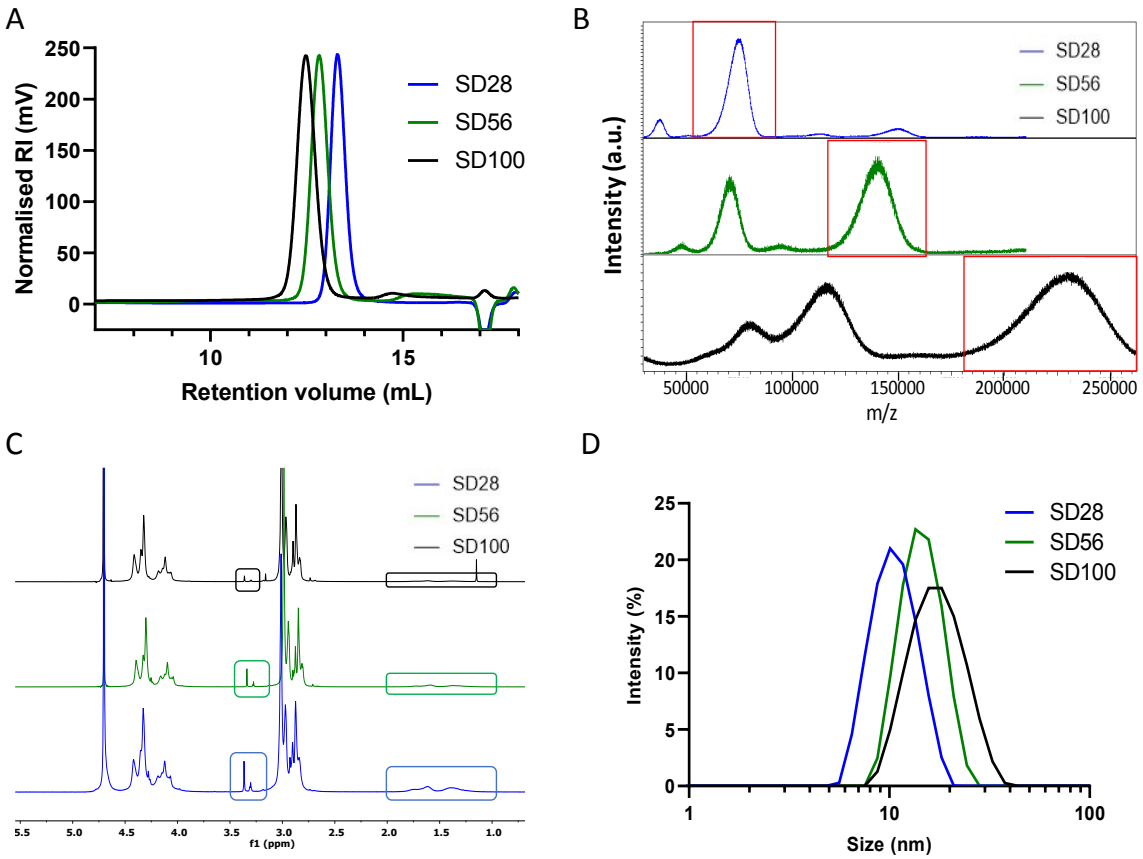

Figure 1. Characterization data for SD28-SD100: (A) aqueous SEC-RI chromatograms, (B) MALDI-TOF-MS spectra, (C) ^{1}HNMR (D_2O) with highlighted signals from lysine dendrimer core (1.0 -1.9 ppm) and chain end methoxy groups (3.2 -3.4 ppm), (D) hydrodynamic sizes determined from DLS (intensity, in PBS).

Mass photometry for characterization of star polymers. Interferometric scattering mass spectrometry, also referred to as mass photometry is a novel technology that allows rapid mass characterization of proteins under native conditions.[38] The

technology is based on interferometric scattering microscopy of individual molecules in direct proximity of an interface, where interferometric contrast has been shown to be linearly proportional to mass within a mass range (40 kDa - 4000 kDa).[38] Mass photometry has so far been applied almost exclusively in the context of protein samples. Here, we extended the utility of mass photometry and explored the characterization of the star polymers. The PSar star polymers represented good candidates, given that the molar masses of these polymers were within the measurement range of the instrument and the materials were composed of amino-acid based building blocks.[38] As scattering signal scales with the polarizability, which is a function of the refractive index and proportional to the particle volume, the contrast-to-mass conversion is typically achieved using a native protein ladder with known species of different sizes (supporting information Figure S1). The masses obtained for the star polymers were in good agreement with both SEC-TDA and MALDI-TOF-MS despite differences in refractive index between proteins (dn/dc ~0.185) and the PSar star polymers (dn/dc ~0.16 - 0.17) (Figure 2A and Table 1). Given that the instrument measured individual

nanoparticles, the mass average obtained across the number of counts should have been in better agreement with the number average molar masses obtained from SEC-TDA. This appeared to be the case, where the masses obtained for SD28 and SD56 fitted exactly with the SEC-TDA data. The exception was with the largest star polymer, SD100 where the mass found from mass photometry was 24 kDa lower than the number average molar mass determined by SEC-TDA, albeit within error. The technique was also used to follow the progress of the polymerization of a separate sample of SD56, where aliquots of sample mixture were removed and precipitated into ethyl acetate every 30 minutes for 3.5 hours and later measured (Figure 2B + C). The data showed that the polymerization was rapid with a plateauing of molar mass after approximately 1.5 hours. These results were corroborated with MALDI-TOF-MS (Supporting Information Figure S2) showing the same trend, albeit with higher masses.

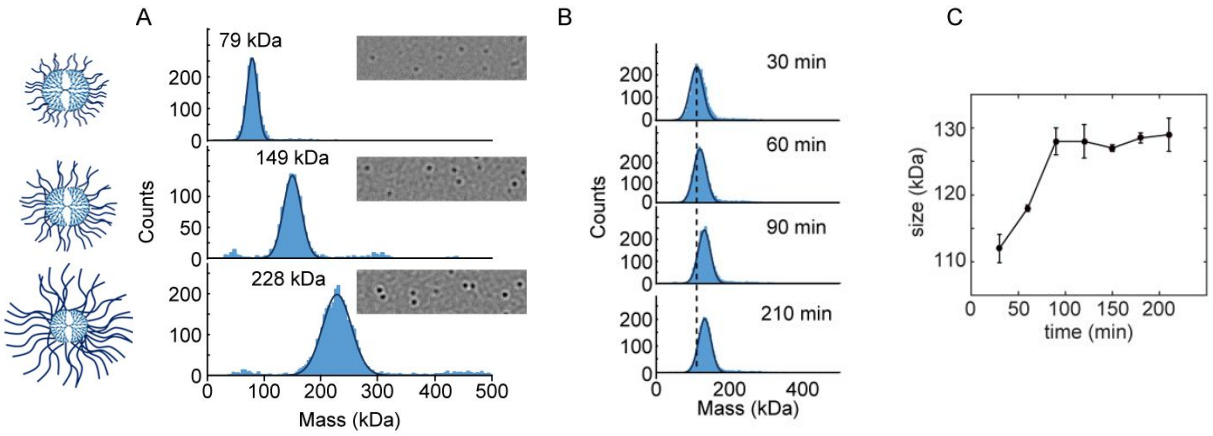

Figure 2. Mass photometry data: (A) different sized star polymers, SD28, SD56 and SD100, (B) time course of the reaction for a separate SD56 sample, (C) plot of the molar mass change over time.

These results reiterate the need to cross-examine samples from multiple analytical techniques to have the most accurate interpretation of the sample. As far as we are aware this is the first application of mass photometry for the characterization of star polymers. Further investigation across different polymer types is warranted to understand limitations, but when considering the speed of the measurements coupled with close mass interpretation, this work highlights that this technique could provide a valuable addition in the field of polymer chemistry and drug delivery.

In vivo plasma pharmacokinetics. As an initial assessment of the star polymers performance *in vivo*, plasma pharmacokinetic data was obtained following intravenous administration to immune-competent mice following a 50 mg/kg dose (Figure 3). To determine the plasma concentrations, the polymers were modified with a Cy5 dye and to prevent rapid clearance from the circulation due to residual amines, the remaining end groups were modified with succinic anhydride to give carboxyl groups, similar to examples previously reported for polyoxazoline-modified dendrimers.[8] The different sized star polymers all demonstrated excellent prolonged circulation times, with times to 50% clearance of the polymers from circulation of 19 h, 40 h and 37 h, and mean terminal half-lives of 51 h, 62 h and 88 h, corresponding to SD28, SD56 and SD100 respectively. Their circulation clearance behavior reflected the differences in hydrodynamic size, where the largest star polymer SD100 (D_H = 18 nm) had slightly slower clearance and a longer terminal half-life than SD56 (D_H = 14 nm) and SD28 (D_H = 10 nm). It has been shown that plasma terminal half lives in rodents have

generally increased with increasing PEGylation of a variety of different dendrimers, either by increasing dendrimer generation and number of PEG chains or increasing the number of repeat units per PEG chain.[7, 35] Having control over the size is particularly useful when applied to different therapies and administration routes and it can be envisaged that the carrier system is tailored to the drug molecule and line of sight rather than a one-size-fits-all approach.

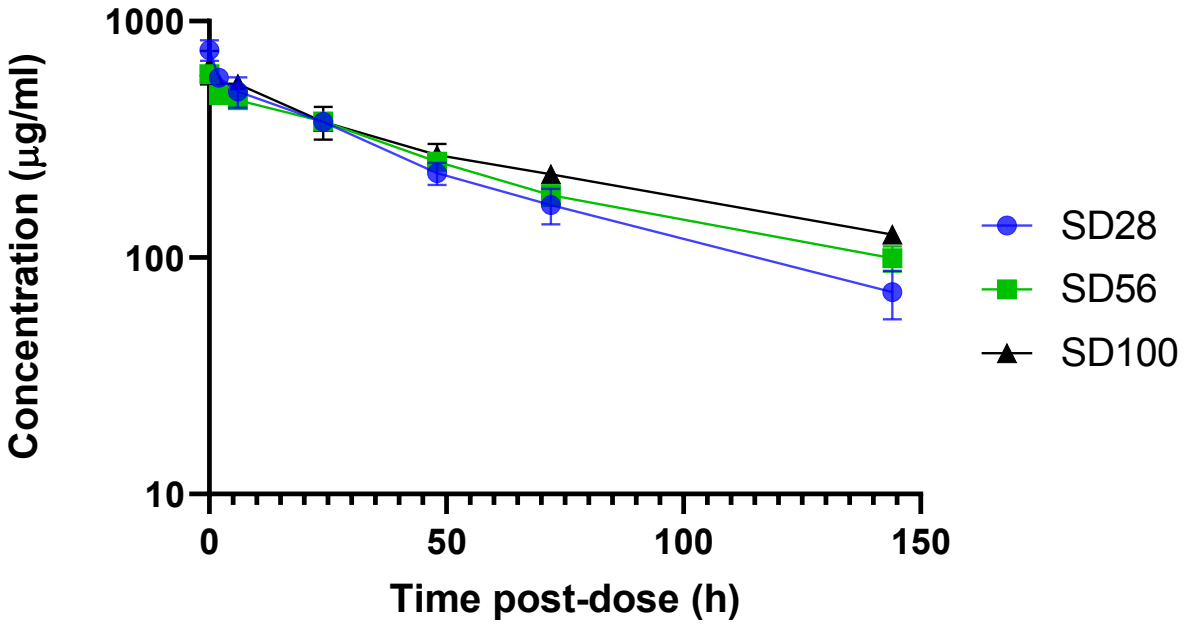

Figure 3. Plasma pharmacokinetic data of Cy5- and carboxyl-functionalized SD28, SD56 and SD100.

***In vivo* efficacy evaluation of SD100-SN38.** To evaluate the platform as a drug delivery system, an *in vivo* efficacy study was performed with an SD100 conjugate of SN-38, a potent topoisomerase inhibitor, and active metabolite of irinotecan. The drug was bound to the star polymer *via* a hydrolytically cleavable ester linker that we have previously reported for this drug but for a polyoxazoline modified star polymer, and was shown to improve efficacy compared to irinotecan and with lower gastrointestinal toxicity.[32] This new conjugate, with a drug release half-life in PBS of 25 h (Supporting Figure S3), was administered intravenously into mice bearing the same subcutaneous colorectal SW620 xenografted tumors as previously described and at the same dose to give good comparison across the technologies. The SD100-SN38 conjugate was dosed at 4 mg/kg of SN-38 (83 mg/kg total conjugate) at weekly dosing intervals for three doses, which was sufficient to cause near-complete tumor regression (Figure 4A). This appeared to be more active than our previous report where four doses of the polyoxazoline star system were required for a similar effect, or total dose of 12 mg/kg vs 16 mg/kg of SN-38. Figure 4B shows the total SN-38 concentrations in tumor, liver and spleen for SD100-SN38 and irinotecan 24 hours after the final dose. This indicated that

the SN-38 contribution from irinotecan had largely been cleared from these tissues due to its rapid clearance following conversion, whilst SN-38 (bound and released) from the polymer was still present. This may be an indication of macrophage uptake of SD100-SN38 in the spleen as well as accumulation and retention in the tumor. It is important to note that these concentrations do not account for the relative organ weight and taking this into account would show higher accumulation in the liver, as the largest organ. As a measure of tolerability, the body weight losses were measured over the dosing period and tumor regrowth phase (Figure 4C). Irinotecan dosed at the maximum tolerated dose of 50 mg/kg IP showed body weight loss of up to 11% of the total body weight. The losses for dosing of SD100-SN38 did not exceed a maximum loss of 3.6% body weight and suggested that it was well tolerated at this efficacious dose.

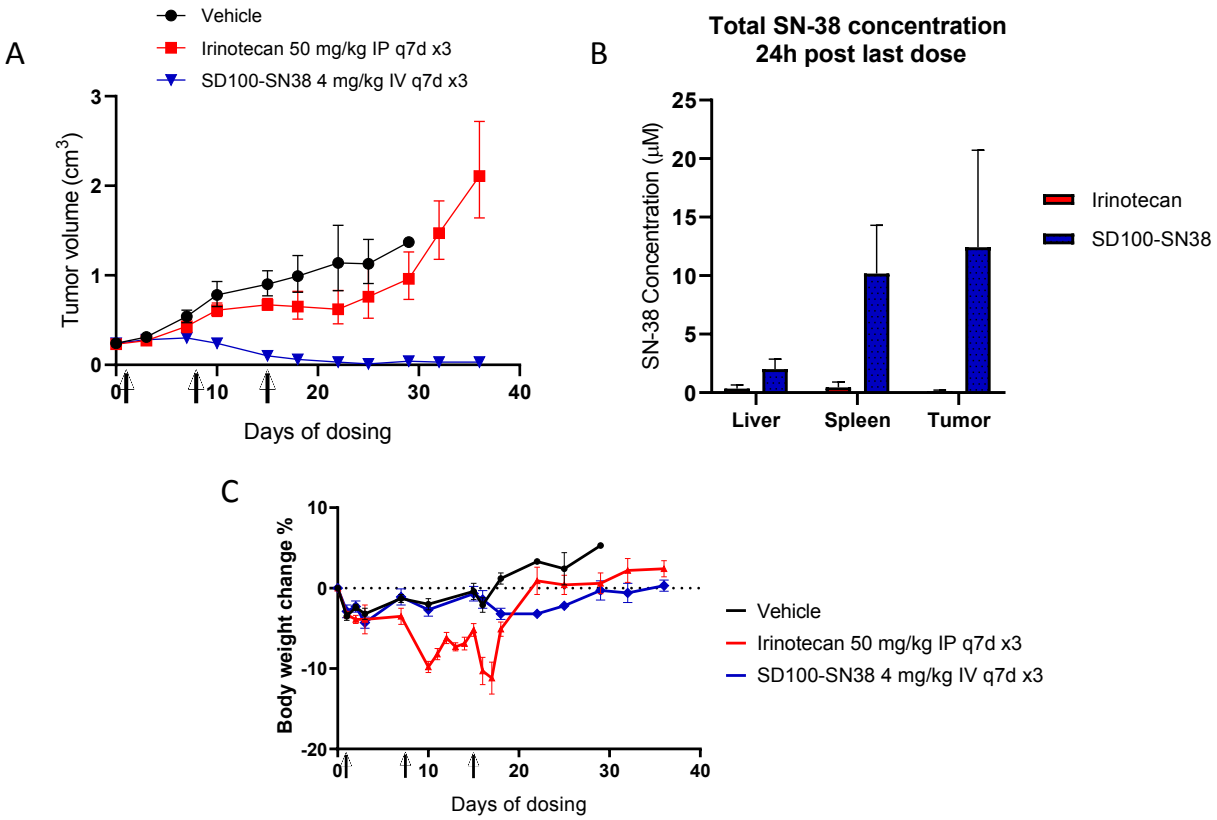

Figure 4. A) Mouse SW620 anti-tumor efficacy plot dosing q7d, n=7. B) SN-38 concentration comparison between liver, spleen and tumor 24 h after final dose n = 3, C) body weight change over time.

SD100 was chosen for this efficacy study owing to the better plasma PK profile compared to the SD56 and SD28, albeit at the cost of drug loading compared to the smaller sized systems (maximum theoretical drug loadings for these systems with this linker and SN-38 would be 12.9 wt.%, 7.5 wt.% and 4.6 wt.% for SD28, SD56 and

SD100, respectively, for 32 molecules of drug per star polymer). Further work is required to understand differences between the different sized star polymers for their drug delivery capabilities, their whole body distributions, and as mentioned, tailoring of the system to best suit the delivery of the therapeutic of interest.

Star polymer chain-end functionalization. An additional benefit of the dendrimer-initiated polymerization was that after full consumption of the monomer, the star polymer had 32 N-termini (secondary amines). The previous examples for SD28, SD56 and SD100 were capped with methoxy groups to mimic some of the more common end groups found for commercial PEG and mono-functional PEG and were intended for use as a passively targeted delivery system. To capitalize on the presence of surface amino groups, another sample of SD56 was prepared and purified directly following the polymerization step without end group capping (^{1}HNMR Supporting Figure S4). This amino-functional star polymer was modified with some commonly reported functional groups that are used for reactions with receptor-targeted ligands. The functional groups included: dibenzylcyclooctyne

(DBCO) (for copper-free “click” chemistry), furfuryl (diels-alder “click”), maleimide (thiol-maleimide “click”) and an additional example of direct biotin modification, all of which were characterized by ^{1}HNMR (Figure 5) and quantified (Supporting Information Table 1). In this example, the end group modification was performed in a second experiment to exemplify various functionalizations, although in future experiments the chain-end modifications could be performed very simply in a one-pot reaction after full consumption of the monomer.

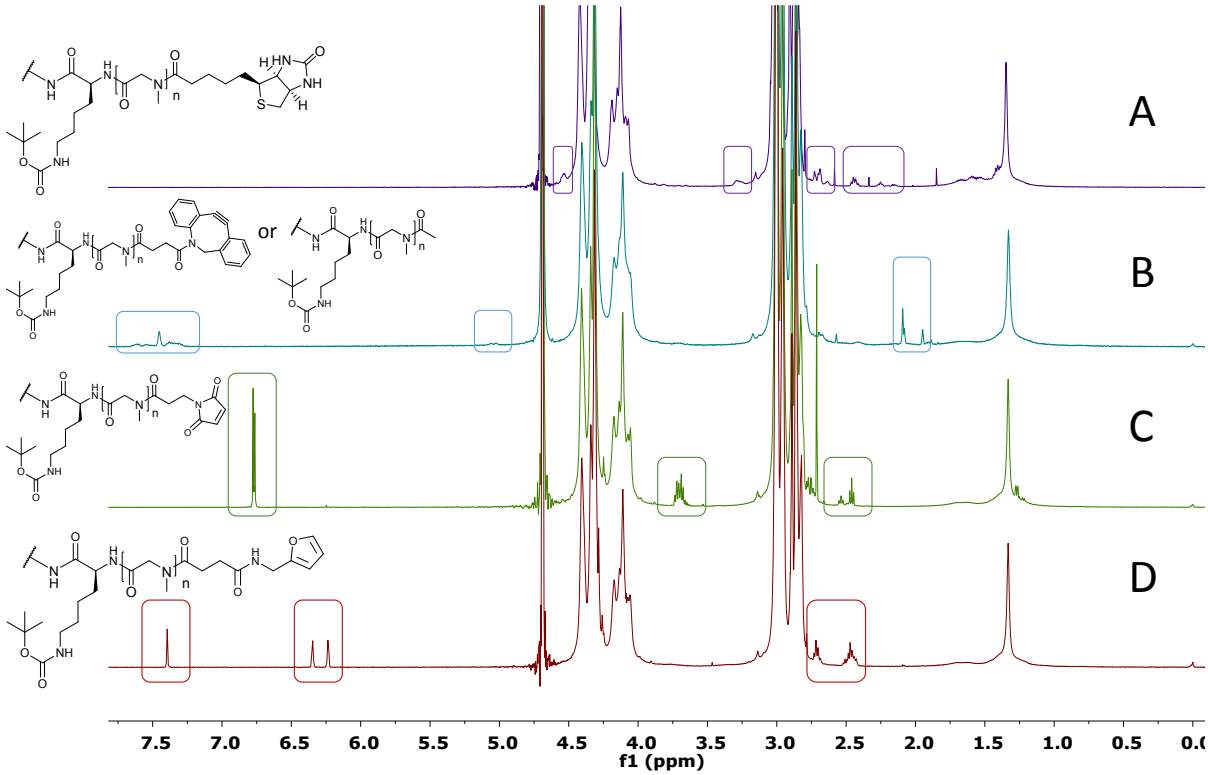

Figure 5. 500MHz ^{1}HNMR of functionalized star polymer SD56Boc. A) biotin, B) DBCO and acetyl groups, C) maleimide, D) furfuryl group.

CONCLUSIONS

L-lysine dendrimer-based 32-arm star polymers were synthesized by the polymerization of sarcosine N-carboxyanhydride from a generation-5 lysine dendrimer macroinitiator to give well-defined materials with versatile properties, which were designed for future drug delivery applications. The molar masses of the star polymers were easily controlled by the feed ratio of dendrimer to monomer, and star polymers of 79 kDa, 149 kDa and 252 kDa were synthesized. Consequently, the hydrodynamic sizes of the star polymers were easily tuned by the molar mass, which is an advantageous feature for nanomedicine design. The different sized star polymers were tested for their plasma pharmacokinetics after intravenous administration in mice and all showed prolonged plasma circulation

times and a size-dependent trend for improved circulation retention was observed in the order of highest to lowest molar mass/ hydrodynamic size. To evaluate the technology for drug delivery, we conjugated the drug molecule SN-38 *via* a hydrolytically cleavable linker and performed an *in vivo* efficacy study in SW620 tumor bearing mice. The results of this showed that a vast improvement in therapeutic index was achieved for the star polymer drug conjugate compared to the prodrug, irinotecan. As a build for next generations of this technology, the polysarcosine N-termini were functionalized with a variety of useful functional groups commonly used for conjugating targeting ligands to demonstrate that this system could have use for receptor mediated drug delivery. Finally, mass photometry, a relatively new characterization technique was introduced for the molar mass determination of these star polymers and compared with SEC-TDA and MALDI-TOF-MS showing good comparison and revealing it and may be a useful technique in the field going forward.

ASSOCIATED CONTENT

Supporting Information. Synthetic methods for L-lysine dendrimer synthesis, Mass Photometry calibration curve plot, MALDI-TOF-MS spectra for reaction monitoring experiment, ^{1}H NMR of SD56Boc prior to end group functionalization. Release rate data in PBS for SD100-SN38 conjugate.

AUTHOR INFORMATION

Corresponding Author

*E-Mail: Richard.England@astrazeneca.com

Author Contributions

The manuscript was written through contributions of all authors. All authors have given approval to the final version of the manuscript.

Notes

The authors declare no conflict of interest however are all employees of AstraZeneca.

Acknowledgements

The authors would like to acknowledge Iain Grant (AstraZeneca) for his expert guidance for interpreting the plasma PK data. The authors wish to thank Joanne Wilson and Aaron Smith (AstraZeneca) for performing the analysis of SN-38 concentration in tissues.

REFERENCES

1. Gaspar, R.; Duncan, R., Polymeric carriers: Preclinical safety and the regulatory implications for design and development of polymer therapeutics. *Adv. Drug Delivery Rev.* **2009,** 61, (13), 1220-1231.
2. Duncan, R., Polymer therapeutics at a crossroads? Finding the path for improved translation in the twenty-first century. *J. Drug Target.* **2017,** 25, (9-10), 759-780.
3. Ekladious, I.; Colson, Y. L.; Grinstaff, M. W., Polymer–drug conjugate therapeutics: advances, insights and prospects. *Nat. Rev. Drug Discov.* **2019,** 18, (4), 273-294.
4. Rawal, M.; Singh, A.; Amiji, M. M., Quality-by-Design Concepts to Improve Nanotechnology-Based Drug Development. *Pharm. Res.* **2019,** 36, (11), 153.
5. Ashford, M., Development and Commercialization of Nanocarrier-Based Drug Products. In *Pharmaceutical Nanotechnology: Innovation and Production*, John Wiley and Sons, 2016; pp 697-734.
6. Peng, C.; Huang, Y.; Zheng, J., Renal clearable nanocarriers: Overcoming the physiological barriers for precise drug delivery and clearance. *J. Control. Release* **2020,** 322, 64-80.

7. Kaminskas, L. M.; Boyd, B. J.; Porter, C. J., Dendrimer pharmacokinetics: the effect of size, structure and surface characteristics on ADME properties. *Nanomedicine (London, U. K.)* **2011,** 6, (6), 1063-84.

8. England, R. M.; Moss, J. I.; Hill, K. J.; Elvevold, K.; Smedsrød, B.; Ashford, M. B., Evaluating liver uptake and distribution of different poly(2-methyl-2-oxazoline) modified lysine dendrimers following intravenous administration. *Biomater. Sci.* **2019,** 7, (8), 3418-3424.

9. Alberg, I.; Kramer, S.; Schinnerer, M.; Hu, Q.; Seidl, C.; Leps, C.; Drude, N.; Möckel, D.; Rijcken, C.; Lammers, T.; Diken, M.; Maskos, M.; Morsbach, S.; Landfester, K.; Tenzer, S.; Barz, M.; Zentel, R., Polymeric Nanoparticles with Neglectable Protein Corona. *Small* **2020,** 16, (18), 1907574.

10. Zhang, P.; Sun, F.; Liu, S.; Jiang, S., Anti-PEG antibodies in the clinic: Current issues and beyond PEGylation. *J. Control. Release* **2016,** 244, 184-193.

11. Birke, A.; Ling, J.; Barz, M., Polysarcosine-containing copolymers: Synthesis, characterization, self-assembly, and applications. *Prog. Polym. Sci.* **2018,** 81, 163-208.

12. Viricel, W.; Fournet, G.; Beaumel, S.; Perrial, E.; Papot, S.; Dumontet, C.; Joseph, B., Monodisperse polysarcosine-based highly-loaded antibody-drug conjugates. *Chem. Sci.* **2019,** 10, (14), 4048-4053.

13. Hu, Y.; Hou, Y.; Wang, H.; Lu, H., Polysarcosine as an Alternative to PEG for Therapeutic Protein Conjugation. *Bioconjug. Chem.* **2018,** 29, (7), 2232-2238.

14. Sano, K.; Ohashi, M.; Kanazaki, K.; Makino, A.; Ding, N.; Deguchi, J.; Kanada, Y.; Ono, M.; Saji, H., Indocyanine Green-Labeled Polysarcosine for in Vivo Photoacoustic Tumor Imaging. *Bioconjug. Chem.* **2017,** 28, (4), 1024-1030.

15. Ueda, M.; Seo, S.; Nair, B. G.; Müller, S.; Takahashi, E.; Arai, T.; Iyoda, T.; Fujii, S.-i.; Tsuneda, S.; Ito, Y., End-Sealed High Aspect Ratio Hollow Nanotubes Encapsulating an Anticancer Drug: Torpedo-Shaped Peptidic Nanocapsules. *ACS Nano* **2019,** 13, (1), 305-312.

16. Klein, P. M.; Klinker, K.; Zhang, W.; Kern, S.; Kessel, E.; Wagner, E.; Barz, M., Efficient Shielding of Polyplexes Using Heterotelechelic Polysarcosines. *Polymers* **2018,** 10, (6), 689.

17. Chen, Y.; Xu, Z.; Zhu, D.; Tao, X.; Gao, Y.; Zhu, H.; Mao, Z.; Ling, J., Gold nanoparticles coated with polysarcosine brushes to enhance their colloidal stability and circulation time in vivo. *J. Colloid Interface Sci.* **2016,** 483, 201-210.
18. Bleher, S.; Buck, J.; Muhl, C.; Sieber, S.; Barnert, S.; Witzigmann, D.; Huwyler, J.; Barz, M.; Süss, R., Poly(Sarcosine) Surface Modification Imparts Stealth-Like Properties to Liposomes. *Small* **2019,** 15, (50), 1904716.
19. Hara, E.; Ueda, M.; Makino, A.; Hara, I.; Ozeki, E.; Kimura, S., Factors Influencing in Vivo Disposition of Polymeric Micelles on Multiple Administrations. *ACS Med. Chem. Lett.* **2014,** 5, (8), 873-877.
20. Kurihara, K.; Ueda, M.; Hara, I.; Ozeki, E.; Togashi, K.; Kimura, S., Control of in vivo disposition and immunogenicity of polymeric micelles by adjusting poly(sarcosine) chain lengths on surface. *J. Nanopart. Res.* **2017,** 19, (7), 242.
21. Aoi, K.; Motoda, A.; Ohno, M.; Tsutsumiuchi, K.; Okada, M.; Imae, T., Synthesis and Assembly of Amphiphilic Tadpole-Shaped Block Copolymers Based on Poly(amido amine) Dendrimer. *Polym. J.* **1999,** 31, (11), 1071-1078.
22. Matsui, H.; Ueda, M.; Hara, I.; Kimura, S., Precise control of nanoparticle surface by host–guest chemistry for delivery to tumor. *RSC Adv.* **2015,** 5, (45), 35346-35351.
23. Aoi, K.; Katsube, M.; Tsutsumiuchi, K.; Okada, M., Controlled Architecture of Nano-Structures Based on Star Dendrimers. *Kobunshi Ronbunshu* **2002,** 59, (12), 742-752.
24. Kaminskas, L. M.; Boyd, B. J.; Porter, C. J. H., Dendrimer pharmacokinetics: the effect of size, structure and surface characteristics on ADME properties. *Nanomedicine* **2011,** 6, (6), 1063-1084.
25. Skoulas, D.; Stuettgen, V.; Gaul, R.; Cryan, S.-A.; Brayden, D. J.; Heise, A., Amphiphilic Star Polypept(o)ides as Nanomeric Vectors in Mucosal Drug Delivery. *Biomacromolecules* **2020,** 21, (6), 2455-2462.
26. Kostka, L.; Kotrchová, L.; Šubr, V.; Libánská, A.; Ferreira, C. A.; Malátová, I.; Lee, H. J.; Barnhart, T. E.; Engle, J. W.; Cai, W.; Šírová, M.; Etrych, T., HPMA-based star polymer biomaterials with tuneable structure and biodegradability

tailored for advanced drug delivery to solid tumours. *Biomaterials* **2020,** 235, 119728.

27. Etrych, T.; Daumová, L.; Pokorná, E.; Tušková, D.; Lidický, O.; Kolářová, V.; Pankrác, J.; Šefc, L.; Chytil, P.; Klener, P., Effective doxorubicin-based nano-therapeutics for simultaneous malignant lymphoma treatment and lymphoma growth imaging. *J. Control. Release* **2018,** 289, 44-55.

28. Tomalova, B.; Sirova, M.; Rossmann, P.; Pola, R.; Strohalm, J.; Chytil, P.; Cerny, V.; Tomala, J.; Kabesova, M.; Rihova, B.; Ulbrich, K.; Etrych, T.; Kovar, M., The structure-dependent toxicity, pharmacokinetics and anti-tumour activity of HPMA copolymer conjugates in the treatment of solid tumours and leukaemia. *J. Control. Release* **2016,** 223, 1-10.

29. Willner, L.; Jucknischke, O.; Richter, D.; Roovers, J.; Zhou, L. L.; Toporowski, P. M.; Fetters, L. J.; Huang, J. S.; Lin, M. Y.; Hadjichristidis, N., Structural Investigation of Star Polymers in Solution by Small-Angle Neutron Scattering. *Macromolecules* **1994,** 27, (14), 3821-3829.

30. Richter, D.; Jucknischke, O.; Willner, L.; Fetters, L.; Lin, M.; Huang, J.; Roovers, J.; Toporovski, C.; Zhou, L., Scaling properties and ordering phenomena of star polymers in solution. *J. Phys. IV* **1993,** 03, (C8), C8-3-C8-12.

31. England, R. M.; Hare, J. I.; Kemmitt, P. D.; Treacher, K. E.; Waring, M. J.; Barry, S. T.; Alexander, C.; Ashford, M., Polymer Chemistry Enhanced cytocompatibility and functional group content of poly(L-lysine) dendrimers by grafting with poly(oxazolines). *Polymer Chemistry* **2016,** 7, (7), 4609-4617.

32. England, R. M.; Hare, J. I.; Barnes, J.; Wilson, J.; Smith, A.; Strittmatter, N.; Kemmitt, P. D.; Waring, M. J.; Barry, S. T.; Alexander, C.; Ashford, M. B., Tumour regression and improved gastrointestinal tolerability from controlled release of SN-38 from novel polyoxazoline-modified dendrimers. *J. Control. Release* **2017,** 247, 73-85.

33. Luong, D.; Kesharwani, P.; Deshmukh, R.; Mohd Amin, M. C. I.; Gupta, U.; Greish, K.; Iyer, A. K., PEGylated PAMAM dendrimers: Enhancing efficacy and mitigating toxicity for effective anticancer drug and gene delivery. *Acta Biomater.* **2016,** 43, 14-29.

34. Somani, S.; Laskar, P.; Altwaijry, N.; Kewcharoenvong, P.; Irving, C.; Robb, G.; Pickard, B. S.; Dufès, C., PEGylation of polypropylenimine dendrimers: effects on cytotoxicity, DNA condensation, gene delivery and expression in cancer cells. *Sci. Rep.* **2018,** 8, (1), 9410.

35. Mehta, D.; Leong, N.; McLeod, V. M.; Kelly, B. D.; Pathak, R.; Owen, D. J.; Porter, C. J. H.; Kaminskas, L. M., Reducing Dendrimer Generation and PEG Chain Length Increases Drug Release and Promotes Anticancer Activity of PEGylated Polylysine Dendrimers Conjugated with Doxorubicin via a Cathepsin-Cleavable Peptide Linker. *Mol. Pharm.* **2018,** 15, (10), 4568-4576.

36. Kaminskas, L. M.; McLeod, V. M.; Ascher, D. B.; Ryan, G. M.; Jones, S.; Haynes, J. M.; Trevaskis, N. L.; Chan, L. J.; Sloan, E. K.; Finnin, B. A.; Williamson, M.; Velkov, T.; Williams, E. D.; Kelly, B. D.; Owen, D. J.; Porter, C. J. H., Methotrexate-Conjugated PEGylated Dendrimers Show Differential Patterns of Deposition and Activity in Tumor-Burdened Lymph Nodes after Intravenous and Subcutaneous Administration in Rats. *Mol. Pharm.* **2015,** 12, (2), 432-443.

37. Raw, S. A., An improved process for the synthesis of DMTMM-based coupling reagents. *Tetrahedron Lett.* **2009,** 50, (8), 946-948.

38. Young, G.; Hundt, N.; Cole, D.; Fineberg, A.; Andrecka, J.; Tyler, A.; Olerinyova, A.; Ansari, A.; Marklund, E. G.; Collier, M. P.; Chandler, S. A.; Tkachenko, O.; Allen, J.; Crispin, M.; Billington, N.; Takagi, Y.; Sellers, J. R.; Eichmann, C.; Selenko, P.; Frey, L.; Riek, R.; Galpin, M. R.; Struwe, W. B.; Benesch, J. L. P.; Kukura, P., Quantitative mass imaging of single biological macromolecules. *Science* **2018,** 360, (6387), 423-427.

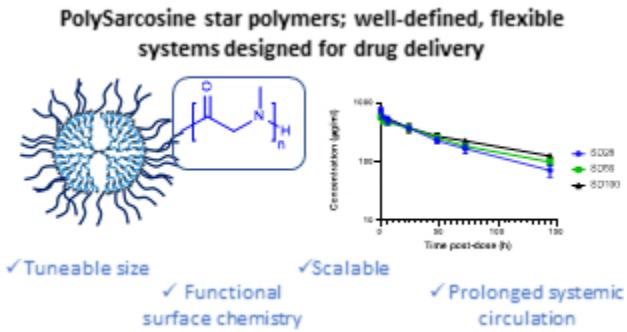

82x44mm (96 x 96 DPI)